Forced Periodic Control of an Exothermic CSTR with Multiple Input Oscillations

Interaction among various oscillating inputs may result in significant modifications in the behavior of a system under forced periodic control. Forced oscillations in the input flow rate and input concentrations of an exothermic continuous stirred tank reactor enable the stabilized operation of the CSTR in the unstable steady state region. Reactor temperature oscillations under forced periodic control are similar to the oscillations resulting from proportional-integral feedback or nonlinear (push-pull) feedback control, and under some operating conditions the oscillation amplitude is significantly lower. Theoretical and experimental studies illustrate the effects of forcing frequency and phase shift on reactor behavior.

Konstantinos Rigopoulos
Xianshu Shu
Ali Çinar
Departments of Chemical and Electrical Engineering
Illinois Institute of Technology
Chicago, IL 60616

Introduction

Forced periodic operation of chemical reactors has been used effectively for conversion improvement, selectivity, and yield enhancement in complex reactions and the stabilization of reactor operation. References to various review papers, different analysis techniques developed, and applications reported are given by Çinar et al. (1987a). Recently there has been a revival of interest in periodically forced systems. Promising experimental results on yield improvement in catalytic reactions have been reported (Cutlip, 1979, Jain et al., 1982; Wilson and Rinker, 1982; Barshad and Gulari, 1985, 1986; Silveston et al., 1986). A technique based on the Carleman linearization of nonlinear plant equations and the maximization of a time-averaged performance measure has been proposed (Lyberatos and Svoronos, 1987) for determining the optimal periodic operation and has been applied to an isothermal reactor model for the selection of the best forcing frequency, amplitude, and waveform. Common features of periodically forced reacting systems, particularly properties of spontaneously oscillating systems that are forced periodically, have been considered (Kevrekidis et al., 1986) and an algorithm using stroboscopic representation has been presented for the numerical computation and stability analysis of invariant tori. In stabilizing reactor operation by periodic forcing, the vibrational control approach has provided successful theoretical and experimental results (Çinar et al., 1987a, b).

Vibrational control (Meerkov, 1982) is a method for modification of the dynamic properties of a system by introducing fast, zero-average oscillations in its parameters. The theory of vibrational control has been developed for linear and nonlinear lumped-parameter systems (Bellman et al., 1983, 1986a, b) using the method of averaging (Bogoliubov and Mitropolsky, 1961). Vibrational control of an exothermic continuous stirred tank reactor (CSTR) by forced oscillations in input flow rate, for stabilized reactor operation has been reported (Çinar et al., 1987a). An application of vibrational control to a laser-illuminated thermochemical system for stabilized system operation has also been presented (Bentsman and Hrostov, 1987).

This study addresses the reactor stabilization problem by forced periodic control with *multiple oscillating inputs.* The preliminary theoretical results (Çinar et al., 1987b) indicated that the interaction of various oscillating inputs may cause significant reductions in output oscillations. Multiple oscillating inputs also enabled the separation of the average concentration and temperature curves, as illustrated in Figure 6). This creates an opportunity for obtaining higher reactor productivity at a given average temperature. In this paper, a comprehensive theoretical analysis and experimental validation of forced periodic control by multiple oscillating inputs are given. As an example system, a CSTR with homogeneous liquid phase exothermic reaction is used and periodic forcing of total input flow rate and of reactant input concentrations is considered. Theoretical and experimental results show that the contribution of the interaction does not always lead to an improvement, and the determination of the phase shift range that causes desirable results is needed.

The effects of multiple oscillating inputs on conversion improvements and selectivity enhancements have also been studied

Correspondence concerning this paper should be addressed to Ali Cinar.

by using the π-criterion approach (Watanabe et al., 1982; Sincic and Bailey, 1980). The contribution of an interaction term that includes explicit dependence on the phase relationship between the inputs has been noted (Sincic and Bailey, 1980). The π-criterion approach permits the consideration of small-amplitude input vibrations. The "vibrational control" approach, on the other hand, enables the analysis of systems subject to high-frequency and large-amplitude input forcing.

In this communication, reactor stabilization experiments using other approaches such as proportional-integral (PI) feedback control and nonlinear feedback control (Bruns and Bailey, 1975, 1977) are also presented. For the test reaction considered in this work, stabilized reactor operation in the unstable steady state region using PI feedback with coolant flow rate manipulation has been reported elsewhere (Chang and Schmitz, 1975a, b). Forced periodic control experiments performed with coolant flow rate oscillations, and PI feedback and nonlinear feedback experiments conducted with reactant flow rate manipulation permit the assessment of all control techniques and manipulated variables considered.

Reactor System

Experimental system

The pilot plant used in earlier studies has been modified to enable simultaneous changes in concentration and total flow rate of input streams while keeping the ratio of reactant concentrations fixed. The reactor system and the dedicated control computer are described in detail by Çinar et al. (1987a). The basic modification is the addition of a third storage tank, Figure 1, which can be used for injecting a water stream at the same temperature as the other reactants to modify the inlet reactant concentrations and the total flow rate. The tubing and control valve (identical to the other valves) that connect this tank to the reactor has also been used for stabilization of reactor operation by vibrating the coolant flow rate. For this mode of operation a 0.375 m long, 6.4 mm (¼ in.) OD stainless steel coil is inserted in the reactor. As the test reaction, the second-order exothermic reaction between sodium thiosulfate ($Na_2S_2O_3$) and hydrogen peroxide (H_2O_2) in aqueous solution is used. For the feed concentration ratio used, the stoichiometric equation for this reaction is:

$$2Na_2S_2O_3 + 4H_2O_2 \rightarrow Na_2S_3O_6 + Na_2SO_4 + 4H_2O$$

The values of various parameters and operating conditions used in theoretical and experimental studies are given in Table 1.

Reactor model with unforced reactant flow rates

The material and energy balances describing the CSTR are:

$$\begin{aligned}
V dc_A/dt' &= F(c_{AF} - c_A) \\
&\quad - V k_0 c_A c_B \exp\{-E/RT'\} \\
V dc_B/dt' &= F(c_{BF} - c_B) \\
&\quad - V k_0 c_A c_B \exp\{-E/RT'\} \\
(m_r C_r + \rho C_P V) dT'/dt' &= \rho C_P F(T_F - T') \\
&\quad + (-\Delta H) V k_0 c_A c_B \exp\{-E/RT'\} + Q \qquad (1)
\end{aligned}$$

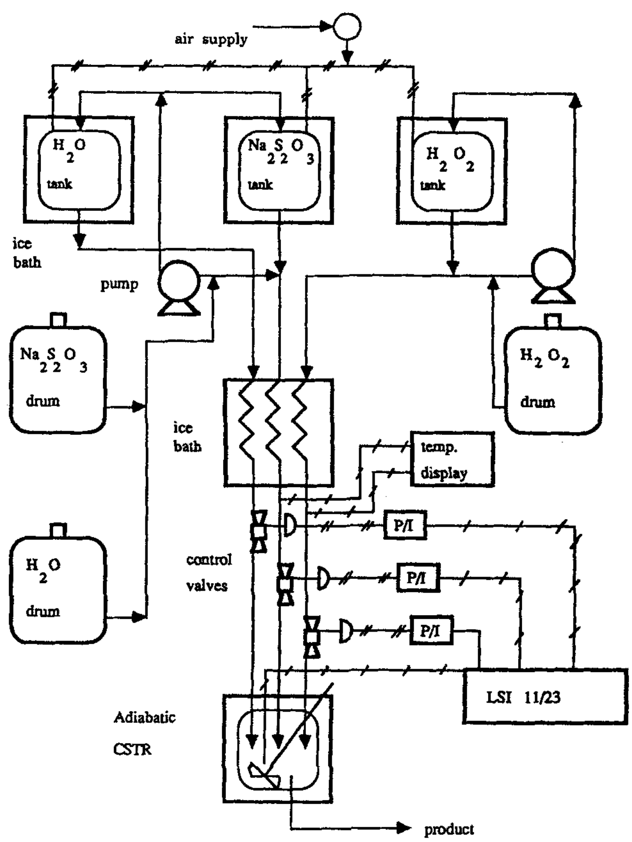

Figure 1. CSTR network.

where c_A and c_B denote the H_2O_2 and the $Na_2S_2O_3$ concentrations, T' is the reactor temperature, t' is the time, and Q is the heat taken by the cooling water. Under adiabatic operation $Q = 0$. When cooling water is used $Q = (H/\rho_c C_{Pc})(T' - T_c)$ where T_c is the coolant temperature and H is the effective heat transfer coefficient expressed by an experimentally determined empirical equation that is a function of coolant flow rate q_c (Rigopoulos, 1986).

Defining the dimensionless variables

$$x_1 = \frac{c_{AF0} - c_A}{c_{AF0}},$$

$$x_2 = \frac{c_{BF0} - c_B}{c_{BF0}},$$

$$x_3 = \frac{T' - T_F}{T_F} \frac{E}{RT_F}$$

$$x_c = \frac{T_c - T_F}{T_F} \frac{E}{RT_F}$$

the dimensionless reactor model for adiabatic operation becomes:

$$\begin{aligned}
dx_1/dt &= -x_1 + Da(1 - x_1)(1 - x_2) \exp\{Q_0(x_3)\} \\
dx_2/dt &= -x_2 + bpDa(1 - x_1)(1 - x_2) \exp\{Q_0(x_3)\} \\
dx_3/dt &= -\lambda x_3 + \lambda B Da(1 - x_1)(1 - x_2) \exp\{Q_0(x_3)\} \qquad (2)
\end{aligned}$$

Table 1. Numerical Values of Parameters and Constants, Operating Conditions

Simulation Studies		Experiments	
c_{Af}	$= 1.2 \times 10^3$ mol/m^3	c_{Af}	$= 1.2 \times 10^3$ mol/m^3
c_{Bf}	$= 0.8 \times 10^3$ mol/m^3	c_{Bf}	$= 0.8 \times 10^3$ mol/m^3
k_o	$= 3.26 \times 10^{13}$ m^3/mol $H_2O_2 \cdot$ s	T_f	$= 273.75 \pm 0.4$ K
$-\Delta H/\rho C_P$	$= 73.2 \times 10^3$ m^{3}K/mol	V	$= 240$ cm^3
E	$= 67.65$ kJ/mol H_2O_2	F_M	$= 45.5$ cm^3/s
T_f	$= 274.1$ K	F_m	$= 2.5$ cm^3/s
$m_r C_r/\rho C_P V$	$= 0.1$	c_{AM}	$= 2.0 \times 10^3$ mol/m^3
		c_{BM}	$= 1.33 \times 10^3$mol/m^3
		c_{Am}	$= c_{Bm} = 0$

where the exponent $1/(1 + x_3/\gamma)$ has been approximated with enough accuracy using $Q_0(x_3) = \Sigma_{k=0}^{4} x_3^{k+1}/(-\gamma)^k$. A discussion of the reactor model with unforced inputs, its experimental validation, and its regions of stability have been presented by Çinar et al. (1987a).

When the coolant flow rate is forced periodically using square wave forcing functions, $q_c = q_{c0}[1 + A_c f_c(\omega' t')]$. The heat transfer coefficient, which is a function of q_c, can be represented as $H = H_0 + A_H f_c(\omega' t')$. Following the procedure of Çinar et al. (1987a) the dimensionless reactor model is obtained:

$$\begin{aligned} dx_1/dt &= -x_1 + Da(1 - x_1)(1 - bpx_1)\exp\{Q_0(x_3)\} \\ dx_3/dt &= -\lambda x_3 + \lambda B Da(1 - x_1)(1 - bpx_1)\exp\{Q_0(x_3)\} \\ &\quad - \lambda d_c Da(x_3 - x_c)[H_0 + A_H f_c(\omega t)]. \end{aligned} \tag{3}$$

Reactor model with multiple periodically forced inputs

Assume that the periodically forced input flow rate is of the form

$$F(t') = F_0[1 + A_F f(\omega' t')] \tag{4}$$

and the periodically forced reactant feed concentrations are of the form

$$\begin{aligned} c_{AF}(t') &= c'_{AF0}[1 + A_C f(\omega' t' + 2\pi\sigma)] \\ c_{BF}(t') &= c'_{BF0}[1 + A_C f(\omega' t' + 2\pi\sigma)] \end{aligned} \tag{5}$$

where A_F and A_C denote the amplitude, c'_{AF0} and c'_{BF0} are the average input concentrations at constant flow rate, ω' is the frequency of oscillation, and σ is the phase shift between the flow rate and concentration oscillations. In this study the concentration oscillations will be generated at the same instant and the frequency of concentration and flow rate oscillations will be the same. Periodic forcing of other input combinations, such as coolant flow rate (or coolant temperature) and one reactant input concentration, or two reactant input concentrations with phase shift, have not been considered because variations in the ratio of reactant feed concentrations cause side reactions (Deng, 1985) that are not represented by the reactor model. The occurrence of side reactions is easily determined experimentally due to the formation of H_2S. The nonsymmetric rectangular waveform, Figure 2, which generates the optimal shape of oscillations for linear systems (Meerkov, 1980) is used as the forcing function. Hence, $f(\omega' t')$ is defined by

$$f(\omega' t') = \begin{cases} 1 - \alpha, & \text{if } (2n - \alpha/2)\pi < |\omega' t'| < (2n + \alpha/2)\pi \\ -\alpha, & \text{if } (2n + \alpha/2)\pi < |\omega' t'| < (2n + 2 - \alpha/2)\pi \\ 0, & \text{otherwise} \end{cases} \tag{6}$$

where α is the duty fraction and $n = 0, 1, 2, \ldots$. The flow rate is shifting between a high value, F_M, and a low value, F_m. Similarly, the reactant inlet concentrations take two values; for reactant A, c_{AFM} and c_{AFm}. The Fourier series expansion of $f(\omega' t')$ is

$$f(\omega' t') = \sum_{k=1}^{\infty} \beta'_k \cos k\omega' t'$$

where $\beta'_k = (2/k\pi)\sin \alpha k\pi \ \forall\ k = 1, 2, \ldots$.

Since the input flow rate and concentrations are changing at different instants (which are out of phase) the average input concentration, c_{AF0}, over a period T must be defined using

$$c_{AF0} = \frac{1}{TF_0}\int_0^T c_{AF}(\omega' t')F(\omega' t')\, dt'$$

This average c_{AF0} can be expressed in terms of the average input concentration at constant flow rate, $c'_{AF0} = (1/T)\int_0^T c_{AF}(\omega' t')\, dt'$ and a multiplier k_{fc} as $c'_{AF0} = k_{fc} c_{AF0}$, where

$$k_{fc} = \begin{cases} 1/[\alpha(A_F + A_C) - (\sigma + 2\alpha^2)A_F A_C], & \text{if } \alpha > \sigma > 0 \\ 1/[1 - \alpha^2 A_F A_C], & \text{if } \sigma > \alpha > 0 \\ 1/[\alpha(A_F + A_C) - (2\alpha^2 - \sigma)A_F A_C], & \text{if } \alpha > -\sigma > 0 \end{cases}$$

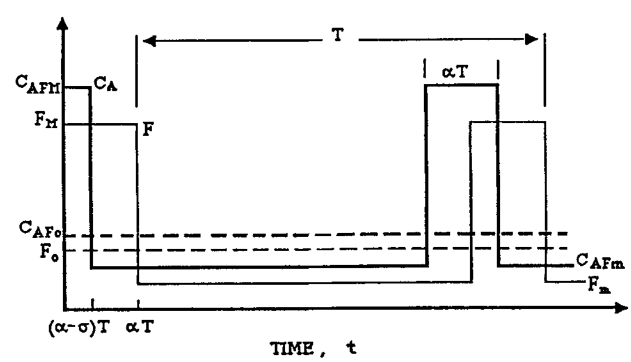

Figure 2. Nonsymmetric rectangular pulse.

The reactor system with input flow rate oscillations in the form of Eq. 4 and input concentration oscillations in the form of Eqs. 5 is described by

$$
\begin{aligned}
V dc_A/dt' &= F_0[1 + A_F f(\omega' t')] \\
&\quad \cdot \{c_{AF0} - c_A + (k_{fc} - 1)c_{AF0} \\
&\quad + k_{fc} c_{AF0} A_C f(\omega' t' - 2\pi\sigma)\} \\
&\quad - V k_0 c_A c_B \exp\{-E/RT'\} \\
V dc_B/dt' &= F_0[1 + A_F f(\omega' t')] \\
&\quad \cdot \{c_{BF0} - c_B + (k_{fc} - 1)c_{BF0} \\
&\quad + k_{fc} c_{BF0} A_C f(\omega' t' - 2\pi\sigma)\} \\
&\quad - V k_0 c_A c_B \exp\{-E/RT'\} \\
(m_r C_r + \rho C_p V) dT'/dt' &= \rho C_p F_0 [1 + A_F f(\omega' t')] \\
&\quad \cdot (T_F - T') + (-\Delta H) V k_0 c_A c_B \\
&\quad \cdot \exp\{-E/RT'\} \qquad (7)
\end{aligned}
$$

The corresponding dimensionless equations are

$$
\begin{aligned}
dx_1/dt &= -[1 + A_F f(\omega t)]x_1 \\
&\quad + f_1(\omega t) + Da(1 - x_1)(1 - x_2)\exp\{Q_0(x_3)\} \\
dx_2/dt &= -[1 + A_F f(\omega t)]x_2 + f_1(\omega t) \\
&\quad + bpDa(1 - x_1)(1 - x_2)\exp\{Q_0(x_3)\} \\
dx_3/dt &= -\lambda[1 + A_F f(\omega t)]x_3 \\
&\quad + \lambda B Da(1 - x_1)(1 - x_2)\exp\{Q_0(x_3)\} \qquad (8)
\end{aligned}
$$

where $Q_0(x_3) = \Sigma_{k=0}^{4} x_3^{k+1}/(-\gamma)^k$,

$$
\begin{aligned}
f_1(\omega t) &= (1 - k_{fc})A_F \sum_{k=1}^{\infty} \beta'_k \cos k\omega t \\
&\quad - k_{fc} A_C \sum_{k=1}^{\infty} \beta'_k \cos k(\omega t - 2\pi\sigma) \\
&\quad - k_{fc} A_F A_C \sum_{k=1}^{\infty} (\mu_k \sin k\omega t + \nu_k \cos k\omega t) \qquad (9)
\end{aligned}
$$

and

$$
\mu_k = \begin{cases}
[-\cos \alpha k\pi + (1 - \alpha)\cos(2\sigma - \alpha)k\pi + \alpha \cos(2\sigma + \alpha)k\pi]/k\pi & \text{if } \alpha > \sigma > 0 \\
\alpha[\cos(2\sigma + \alpha)k\pi - \cos(2\sigma - \alpha)k\pi]/k\pi & \text{if } \sigma > \alpha > 0 \\
[(\alpha - 1)\cos(2\sigma + \alpha)k\pi + \cos \alpha k\pi - \alpha \cos(2\sigma - \alpha)k\pi]/k\pi & \text{if } \alpha > -\sigma > 0
\end{cases}
$$

$$
\nu_k = \begin{cases}
[(1 - 2\alpha)\sin \alpha k\pi + (\alpha - 1)\sin(2\sigma - \alpha)k\pi - \alpha \sin(2\sigma + \alpha)k\pi]/k\pi & \text{if } \alpha > \sigma > 0 \\
\alpha[\sin(2\sigma - \alpha)k\pi - 2\sin \alpha k\pi - \sin(2\sigma + \alpha)k\pi]/k\pi & \text{if } \sigma > \alpha > 0 \\
[(1 - \alpha)\sin(2\sigma + \alpha)k\pi + (1 - 2\alpha)\sin \alpha k\pi + \alpha \sin(2\sigma - \alpha)k\pi]/k\pi & \text{if } \alpha > -\sigma > 0
\end{cases}
$$

Asymptotic Analysis

The averaged equations for the reactor system with periodically forced inputs are developed using the method outlined in the appendix of Çinar et al. (1987a). The averaged Eqs. 13 given here permit direct computation of the cycle average temperature and concentration of the stationary cycling states. Hence, long computations involving transient simulations until a stationary cycling state is reached followed by the calculation of cycle averages are eliminated.

Reactor system with multiple periodically forced inputs

Let $\epsilon = 1/T_r\omega$, $\theta = t/\epsilon$, and $\alpha_F = \epsilon A_F$, where T_r is the dynamical response time constant of the reactor. The system with multiple periodically forced inputs, Eqs. 8, can then be rewritten as

$$\dot{x} = \epsilon X_1(x, \theta) + \alpha_F X_2(x, \theta) \qquad (10)$$

where

$$x = [x_1, x_2, x_3]^T$$

$$
X_1(x, \theta) = \begin{bmatrix}
-x_1 + f_1(\theta/T_r) + Da(1 - x_1)(1 - x_2)\exp\{Q_0(x_3)\} \\
-x_2 + f_1(\theta/T_r) + bpDa(1 - x_1)(1 - x_2)\exp\{Q_0(x_3)\} \\
-\lambda x_3 + \lambda B Da(1 - x_1)(1 - x_2)\exp\{Q_0(x_3)\}
\end{bmatrix}
$$

and

$$
X_2(x, \theta) = \begin{bmatrix}
-f(\theta/T_r)x_1 \\
-f(\theta/T_r)x_2 \\
-\lambda f(\theta/T_r)x_3
\end{bmatrix}
$$

After solving the following generating equation,

$$dx/d\theta = X_2(x, \theta) \qquad (11)$$

the expressions that will be used in substitutions are found:

$$
\begin{aligned}
x_1 &= y_1 \exp\left\{-\alpha_F \sum_{k=1}^{\infty} \beta_k \sin k\theta\right\} \\
x_2 &= y_2 \exp\left\{-\alpha_F \sum_{k=1}^{\infty} \beta_k \sin k\theta\right\} \\
x_3 &= y_3 \exp\left\{-\lambda\alpha_F \sum_{k=1}^{\infty} \beta_k \sin k\theta\right\} \qquad (12)
\end{aligned}
$$

Substituting Eqs. 12 into Eq. 10 and averaging Eq. 10 over the fast time θ, the averaged equations are obtained:

$$
\begin{aligned}
\dot{z}_1 &= -z_1 + S + Da \exp\{Q_0(z_3)\} \\
&\quad \cdot [1 + \gamma_a^2\{[\lambda Q_1(z_3) - 1]^2 + \lambda^2 Q_2(z_3)\} \\
&\quad + \gamma_\sigma[Q_1^2(z_3) + Q_2(z_3)] - (z_1 + z_2) \\
&\quad \cdot \{1 + \lambda^2\gamma_a^2[Q_1^2(z_3) + Q_2(z_3)]\} \\
&\quad + z_1 z_2(1 + \gamma_a^2\{[\lambda Q_1(z_3) + 1]^2 \\
&\quad + \lambda^2 Q_2(z_3)\}) + \gamma_\sigma[Q_1^2(z_3) + Q_2(z_3)]]
\end{aligned}
$$

$$
\begin{aligned}
\dot{z}_2 = & -z_2 + S + bpDa \exp\{Q_0(z_3)\} \\
& \cdot [1 + \gamma_\alpha^2\{[\lambda Q_1(z_3) - 1]^2 + \lambda^2 Q_2(z_3)\} \\
& + \gamma_\sigma[Q_1^2(z_3) + Q_2(z_3)] - (z_1 + z_2) \\
& \cdot \{1 + \lambda^2\gamma_\alpha^2[Q_1^2(z_3) + Q_2(z_3)]\} \\
& + z_1 z_2(1 + \gamma_\alpha^2\{[\lambda Q_1(z_3) + 1]^2 \\
& + \lambda^2 Q_2(z_3)\}) + \gamma_\sigma[Q_1^2(z_3) + Q_2(z_3)]] \\
\dot{z}_3 = & -\lambda z_3 + \lambda BDa \exp\{Q_0(z_3)\}\{1 + \gamma_\alpha^2\lambda^2\{[Q_1(z_3) - 1]^2 \\
& + Q_2(z_3)\} + \gamma_\sigma\lambda^2[Q_1^2(z_3) + Q_2(z_3)] - (z_1 + z_2) \\
& \cdot \{1 + \gamma_\alpha^2[\lambda^2 Q_2(z_3) + (\lambda - 1 - \lambda Q_1(z_3))]^2\} \\
& + z_1 z_2[1 + \gamma_\alpha^2(\lambda^2 Q_2(z_3) + [\lambda - 2 - \lambda Q_1(z_3)^2]) \\
& + \gamma_\sigma(2 - \lambda)^2(Q_1^2(z_3) + Q_2(z_3))]\} \qquad (13)
\end{aligned}
$$

where

$$Q_i(z_3) = \sum_{k=0}^{4} (k+1)^i z_3^{k+1}/(-\gamma)^k \quad \forall i = 0, 1, 2$$

$$\gamma_\alpha^2 = \frac{\alpha_F^2}{4}\sum_{k=1}^{\infty}\beta_k^2$$

$$\gamma_\sigma = \frac{\lambda^2\alpha_F^2}{4}\left(\frac{3}{8}\sum_{k=1}^{\infty}\beta_k^4 - 0.5\beta_1^3\beta_3 + 1.5\beta_1^2\beta_2\beta_4 + 3\beta_1\beta_2\beta_3\beta_4\right)$$

$$
\begin{aligned}
S = & (1 - k_{fc})A_F\alpha_F^2/8\sum_{k=1}^{\infty}\beta'_{2k}\beta_k^2 \\
& - k_{fc}A_C\{(\alpha_F^2/8)\sum_{k=1}^{\infty}\beta_k^2\beta'_{2k}\cos 2\pi k\sigma \\
& + (\alpha_F^2/4)\beta'_1(\beta_1\beta_2 + \beta_2\beta_3)\cos 2\pi\sigma \\
& + (\alpha_F/2)\sum_{k=1}^{\infty}\beta_k\beta'_k\sin 2\pi k\sigma\} \\
& - k_{fc}A_F A_C\{(\alpha_F/2)\sum_{k=1}^{\infty}\mu_k\beta_k \\
& + (\alpha_F^2/8)\sum_{k=1}^{\infty}\nu_{2k}\beta_k^2\}
\end{aligned}
$$

and

$$\beta_k = \frac{2}{\pi k^2}\sin\alpha k\pi \quad \forall k = 1, 2, \ldots$$

The steady state equations of the averaged system which approximate the cycle averages of the stationary cycling states are obtained by setting $\dot{z}_1$, $\dot{z}_2$, and $\dot{z}_3$ equal to zero. The steady state characteristics of approximate cycle averages, z_{1S} and z_{3S}/B are shown in Figure 3 for various values of frequency ω and phase shift σ. The dimensionless concentration is represented by the broken lines and the dimensionless temperature (divided by B) by solid lines. These two lines coincide for a given set of parameter values when the reactor is operated with unforced inputs or with forced oscillations in only one input (Çinar et al., 1987a). With two oscillating inputs, changes in the frequency of oscillation alone, Figure 3a, do not result in a large variation in the averaged stationary cycling state profiles when there is no phase shift between inputs. As expected, at higher frequencies the profiles of the cycle averages of the stationary cycling states approach the steady state profile of the system with stationary inputs. Changes in phase shift—Figure 3b, curves 2–5 correspond to $\sigma = -0.05, -0.15, -0.25, -0.35$,—are more effective. As the magnitude of phase shift increases or as the frequency of oscillation is reduced, the profiles of the average system move away from that of the system with unforced inputs and indicate stabilized states in the unstable steady state region of the original system. Stabilized operation in the unstable steady state region of the unforced system indicates that, for a specific average residence time, the temperature and conversion of an unstable steady state of the unforced system can be obtained as stable steady states of the averaged forced system.

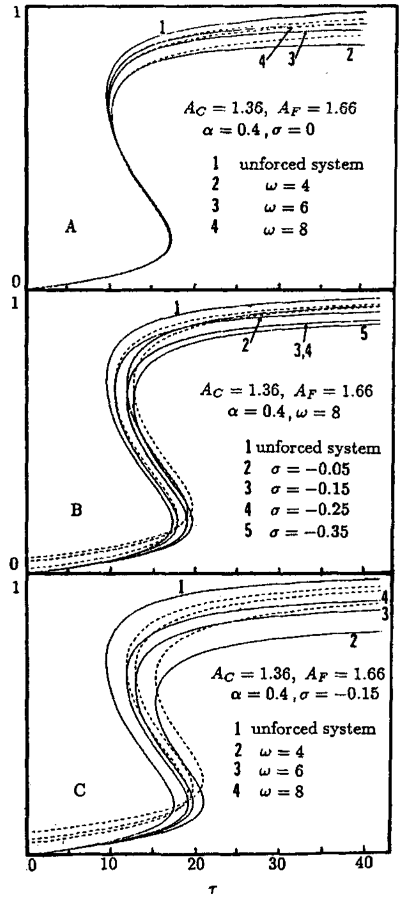

Figure 3. Effects of frequency and phase shift on average steady state characteristics of CSTR.

A. Frequency variation with $\sigma = 0$

B. Phase shift variations

C. Frequency variations at $\sigma = -0.15$. $\alpha > -\sigma > 0$

-------- z_{1S}; z_{3S}/B

The forced periodic stabilization is due to the formation of an asymptotically stable limit cycle instead of the unstable steady state of the system with fixed inputs, such that the average temperature along the limit cycle is arbitrarily close to the temperature of the original unstable state. The average temperature of such a limit cycle and the corresponding average residence time is represented by a point on an S-shaped curve in Figure 3. The stable limit cycle on which the system moves is a result of migration of the upper stable steady state, and not the result of stabilizing the saddle (unstable intermediate) steady state. For a given state (the state variables being the concentration and the temperature of the reacting mixture) the average residence time under forced periodic control may be different than the residence time of the system with fixed inputs. The proximity of the two residence times depends on the operating conditions. For some operating conditions, the upper branch of the average temperature curve intersects the unstable portion of the steady state curve of the system with fixed inputs (Çinar et al., 1987b) and enables forced periodic stabilization at the same residence time.

Previous studies have indicated a lower bound on periodic forcing frequency ($\omega \simeq 2.5$) for the asymptotic analysis to be valid and for reactor temperature oscillation amplitude to be relatively small (Çinar et al., 1987a). For frequencies smaller than the lower bound, the deviations between the cycle averages of the stationary cycling states computed by transient simulations until stationary cycling state is reached followed by the calculation of cycle averages (namely $\overline{x}_{1S}$ and $\overline{x}_{3S}/B$), and the cycle averages computed by solving the steady state equations of the averaged system (namely z_{1S} and z_{3S}/B), are too large. Also, the reactor temperature swings between the upper and lower stable steady state temperatures in a quasisteady-state fashion. Consequently, the forcing frequency must be set to a value greater than the lower bound. Yet, as the forcing frequency is increased the cycle average temperature and concentration profiles approach the steady state profiles of the unforced system and the region for stabilized operation is reduced. Phase shift between periodically forced inputs can lower the upper stable branch of the stationary cycle average profiles and increase the region of stabilized operation at a given forcing frequency. The variation in frequency causes dramatic changes when there is a phase shift, Figure 3c. As σ and α are varied the separation among the average stabilized states curves and the lowering of the upper stable branch are affected, Figure 4. An increase in phase shift σ from -0.15 to -0.20, Figures 4a, b, and a reduction in the duty fraction α from 0.4 to 0.3, Figures 4b, c, enhances the separation. Three different types of phase shift ($\alpha > \sigma > 0$, $\sigma > \alpha > 0$, $\alpha > -\sigma > 0$) have been considered. The first two types affected the relative positions of the concentration and temperature curves in an undesirable fashion, but the third type ($\alpha > -\sigma > 0$) gave promising results for this reactor system.

Other factors, such as the ratio of maximum to minimum flow rate, have also been studied (Çinar et al., 1987b). As the flow rate ratio is increased the average steady state curve moves away from the steady state profile of the system with stationary inputs.

Reactor system with oscillating coolant flow rate

The equations for the averaged system are obtained using the procedure outlined above. For square wave forcing of the coolant flow rate the averaged model equations are:

$$\dot{z}_1 = -z_1 + Da(1 - z_1)(1 - bpz_1)[1 + \xi Q_1^2(z_3)] \exp\{Q_0(x_3)\},$$

$$\dot{z}_3 = -\lambda z_3(1 + \xi)(1 + d_c DaH_0) + \lambda BDa(1 - z_1)(1 - bpz_1)$$
$$[1 + \xi Q_1^2(z_3)] \exp\{Q_0(x_3)\} + x_c d_c DaH_0 \quad (14)$$

where $\xi = [(4\lambda d_c DaA_H/\pi\omega)^2/4]\, \Sigma_{k=0}^{10} (2k - 1)^{-4}$
and Q_0, Q_1 are as defined above.

Periodic forcing in coolant flow rate stabilized reactor operation in the unstable steady state region. For square wave forcing, the average stabilized state profile was slightly shifted to the right and its upper stable branch was lowered, similar in shape to curve 4 in Figure 3a. As before, the stable limit cycle on which the system moves is not due to the stabilization of the saddle (unstable) steady state, but is due to the migration of the upper (stable) steady state.

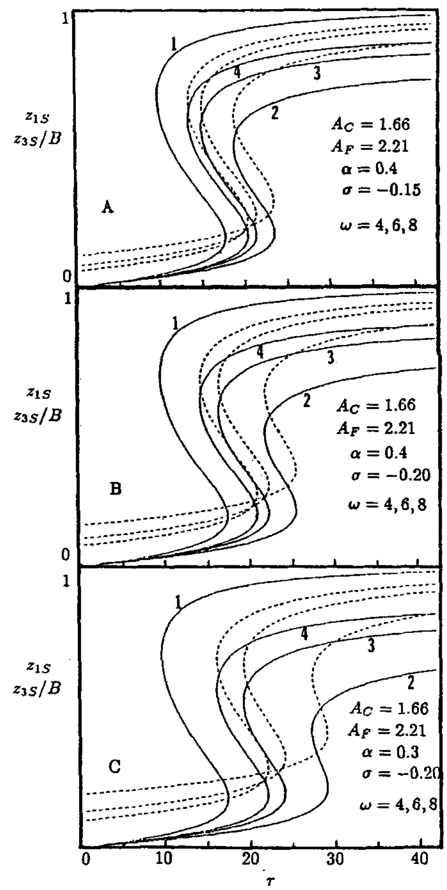

Figure 4. Effects of phase shift and duty fraction variations on average steady state characteristics of CSTR.

$\alpha > -\sigma > 0$
-------- z_{1S}; —: z_{3S}/B
Curves: 1, unforced system; 2, $\omega = 4$; 3, $\omega = 6$; 4, $\omega = 8$

Simulation Results

Simulation studies have been conducted to study the effect of multiple oscillating inputs on the amplitude of reactor temperature swings. The amplitudes of fluctuations in the reactor temperature are reduced to a great extent—Figure 5, temperatures indicated by solid lines—by multiple oscillating inputs. For the case shown, an increase in residence time from 17 to 22 s ($\sigma = -0.15$) or an increase in phase shift magnitude from -0.15 to -0.20 ($\tau = 22$ s) causes slight increases in the amplitude of reactor temperature swings, but a reduction of frequency from 8 to 5 ($\sigma = -0.15$, $\tau = 17$ s) results in a larger amplitude increase. All of these amplitudes are much smaller than the amplitudes observed with single input oscillations in total flow rate (Çinar et al., 1987a).

Another benefit of multiple oscillating inputs is the separation of the average dimensionless concentration and temperature curves, Figure 6. This behavior manifests itself at a different set of parameter values and there is a tradeoff to be made

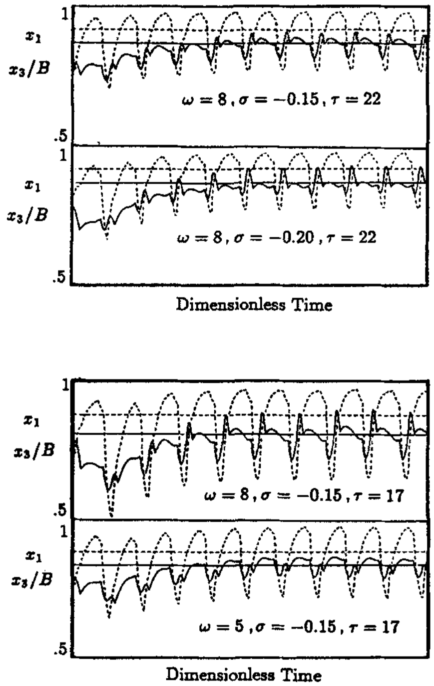

Figure 5. Effects of residence time, phase shift, and frequency on CSTR behavior.

------- xx_1; —: x_3/B

Horizontal lines indicate stationary cycle averages $\bar{x}_{1S}$ and $\bar{x}_{3S}/B$

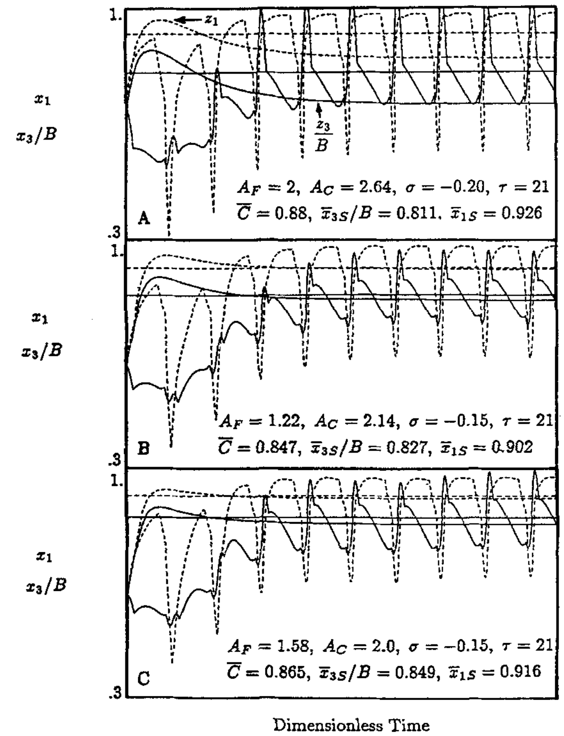

Figure 6. Increase in average conversion $\bar{C}$ under various operating conditions.

$\omega = 6$; $\alpha = 0.3$

------- x_1; —: x_3/B,

Horizontal lines indicate stationary cycle averages $\bar{x}_{1S}$ and $\bar{x}_{3S}/B$

between reduction in temperature swings and improvement of reactor productivity. It is worth noting that the conversion is different than the dimensionless concentration x_1. For the system of Eqs. 8 with input oscillations in the form of Eq. 6, the average conversion, $\bar{C}$, can be expressed as:

$$\bar{C} = \frac{1}{T}\{[1 + (1-\alpha)A_F] \int_{-\alpha T/2}^{\alpha T/2} x_1(t)\,dt + (1 - \alpha A_F) \cdot \int_{\alpha T/2}^{(1-\alpha/2)T} x_1(t)\,dt\} \quad (15)$$

The difference $\Delta C = \bar{C} - \bar{x}_{1S}$ is

$$\Delta C = \alpha A_F\left[\bar{x}_{1S} - \frac{1}{\alpha T}\int_{-\alpha T/2}^{\alpha T/2} x_1(t)\,dt\right] \quad (16)$$

Since the term in brackets in Eq. 16 is the difference between the average value of x_{1S} over a period T and the average value of x_{1S} over αT, when the amplitude A_F is small, the difference ΔC is small. Numerical investigation of this difference has been carried out, and for $\sigma < 0$ when $A_F < 2$, the difference is on the order of 5%. The effects of A_F, A_C, σ, and τ variations on improving reactor productivity are illustrated in Figure 6. Recall that the $\bar{x}_{1S}$ and the $\bar{x}_{3S}/B$ curves (for the z_{1S} and z_{3S}/B curves) coincide for the unforced reactor system and the reactor system with single input forcing (Çinar et al., 1987a). With multiple periodically forced inputs, the two curves are separated from each other, Figures 3 and 4. In Figure 6, the stationary cycle averages $\bar{x}_{1S}$ and $\bar{x}_{3S}/B$ as well as z_{1S} and z_{3S}/B are illustrated for three sets of operating conditions. Also, the numerical values for cycle averages and for the average conversion $\bar{C}$, which is used as a measure of productivity, are listed. For the various cases shown in Figure 6 the values of $\bar{C}$ and $\bar{x}_{3S}/B$ are given in the figure. In all three cases, productivity is slightly higher than that of the unforced or single input forced systems for which $\bar{x}_{1S}$ and $\bar{x}_{3S}/B$ coincide. Note that z_{1S} can be used for $\bar{x}_{1S}$ or $\bar{C}$ without much loss of accuracy for small A_F. Again, phase shift plays an important role in modifying reactor behavior. For example, when σ is reduced from -0.20 to -0.15, Figures 6a, b, for the conditions stated in Figure 6 the difference between $\bar{C}$ and $\bar{x}_{3S}/B$ is reduced by 80%. As expected, the deviation of z_{1S} and z_{3S}/B decreases as the forcing amplitudes are reduced, Figures 6b, c.

Experimental Results

Experiments have been conducted to verify the stabilization of reactor operation and the reduction of amplitude in reactor temperature swings. The conditions leading to separation of the average conversion line caused crystallization of the $Na_2S_2O_3$ solution in the feed lines and the control valve, consequently experiments of this type have not been performed. Experiments have also been carried out for stabilizing reactor operation by oscillating the flow rate of a coolant stream, by proportional-integral feedback control and by nonlinear feedback (push-pull) control by manipulating the feed flow rates. These experiments permit a comparison of the various forced periodic control and feedback control strategies. Theoretical studies and simulations conducted with feedback control strategies (Rigopoulos, 1986) are in agreement with the experimental results summarized in this section.

Coolant flow rate oscillations

Stabilized operation of the CSTR and this test reaction has been achieved in earlier studies (Chang and Schmitz, 1975). Although forced periodic control using coolant flow rate as a manipulated variable does not offer any economic advantage, the experiments illustrate that this approach stabilized reactor operation as well. Theoretical studies indicate that coolant flow rate oscillations move the average stabilized state curve to the right. Experimental results, Figure 7, confirm this shift: At $\tau = 15$ s, $\bar{x}_{3S}/B = 0.85, 0.88$ for $\omega = 3, 6$, respectively. In all cases shown, the system was at the upper stable steady state initially and a square wave pulse shifting between 1 and 15 mL/s has been used. At $\tau = 10$ s the system with stationary inputs is at its upper steady state, but the system under forced periodic control converges to the lower steady state, Figure 7, even when the initial temperature in the reactor is 353 K. The amplitude of the swings in reactor temperature is relatively small and decreases with increasing oscillation frequency, Figure 7.

Proportional-integral feedback control

Proportional-integral (PI) control of the CSTR with total input flow rate as the manipulated variable stabilized reactor operation at an unstable state. In simulation studies, large controller gains and integral time constants ($K_c = 7$, $\tau_I = 10$) resulted in high-frequency, small-amplitude sustained oscillations in reactor temperature. Lower controller settings ($K_c = 1$, $\tau_I = 0.9$) eliminated the limit cycle and resulted in an underdamped response without any steady state offset. Experiments at open-loop unstable set point values ($T = 303, 323$ K), Figure 8, confirmed the limit cycles but the underdamped response approaching a steady state value was not attained. The nonlinearity of the system and the existence of variable process gain are displayed by the modification of the limit cycle as the set point is modified from 323 to 303 K, Figure 8a. If the set point change is large, retuning of controller settings is necessary. The control becomes an on/off action with a frequency similar to that of vibrational control applications. The PI controller handles disturbances well. Two types of disturbances were introduced:

1. Direct addition of 240 mL of water at 278.5 K to the reactor (100% of reacting volume)
2. Full opening of the H_2O_2 valve for 20 s.

The response to opening the valve is given in Figure 8b. The response to water addition is similar except for a sharper reduction in the reactor temperature after the introduction of the disturbance.

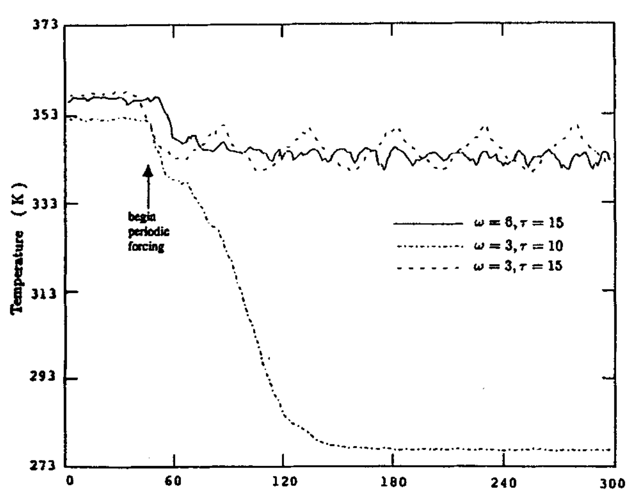

Figure 7. Forced periodic control of CSTR with coolant flow rate oscillations.

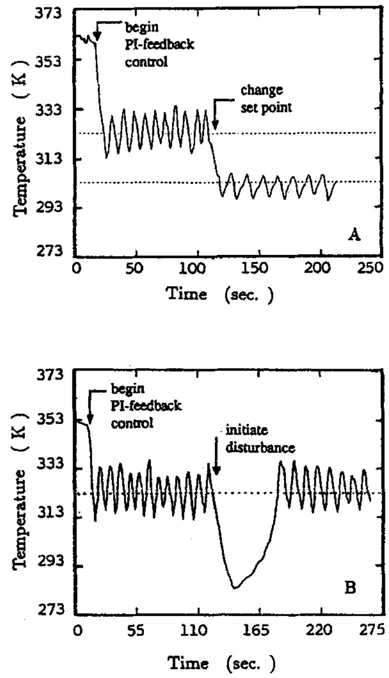

Figure 8. PI feedback control of the CSTR.
A. Effect of set point modifications
B. Effect of disturbances
-------- set point values

Nonlinear feedback control

Stabilized reactor operation can be achieved by generating a small-amplitude stable limit cycle around the desired (unstable) operating point, using a relay with hysteresis as a feedback controller. The design of the relay and the approximate solutions for this mode of operation can be obtained by describing function analysis or by Tsypkin's method (Bruns and Bailey, 1975, 1977). Theoretical studies using Tsypkin's technique and transient simulations indicated that nonlinear feedback control would be successful in stabilizing the exothermic CSTR (Rigopoulos, 1986). To illustrate the operation of the control system, suppose that the control objective is to maintain the reactor temperature within an admissible region N of T^*, Figure 9a. To accomplish this goal, two different feed flow rates corresponding to residence times τ^- and τ^+, which yield the unstable states P^- and P^+ at temperatures T^+ and T^-, are selected. Assume that at a given instant the residence time is set to τ^- and the reactor temperature T lies somewhere in the interval T_s^+ and T_s^-, the upper and lower switching temperatures. When $\tau = \tau^-$ the heat removal by flow is less than the heat generation by reaction in this region N and the reactor temperature would increase to

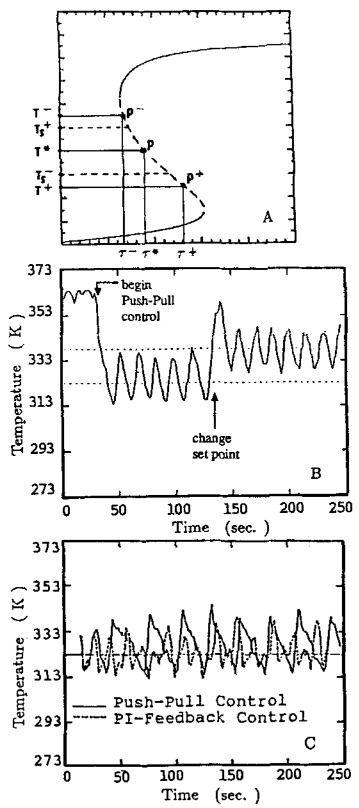

Figure 9. Push-pull (nonlinear feedback) control.

A. Operation principle
B. Effect of set point changes
C. Comparison of push-pull control and PI feedback control at same set point
Horizontal -------- in B and C indicate set point values

reach the equilibrium point P^-. If the residence time is switched by the controller to τ^+ when T reaches the value T_s^+ ($T_s^+ < T^-$), the heat removal will become larger than the heat generation, initiating the reduction of T. When the reactor temperature is reduced to $T = T_s^-$ ($T_s^- > T^+$), τ is set to τ^- again. By alternating between τ^+ and τ^- as the reactor temperature reaches T_s^+ and T_s^-, the process state is pushed and pulled repeatedly by the unstable steady states P^- and P^+ and a limit cycle around T^* is generated.

Experiments have been conducted to study the minimum interval of switching temperatures and the effect of set point changes and disturbances. Reduction of the switching temperature interval to a value smaller than 5 K did not result in further reductions of the amplitude in reactor temperature swings. For a set point of 323 K the amplitude was about 20 K; for the lower set point temperatures both the amplitude of temperature swings and the frequency of oscillation were smaller, Figure 9b. Responses to disturbances have similar shape to those of the CSTR with PI controller, Figure 8b, but recovery duration was twice to three times longer. A comparison of the two feedback techniques, Figure 9c, shows that the PI controller causes oscillations with a frequency almost twice as high as that of nonlinear feedback. This is expected since the PI controller takes action whenever there is a deviation from the set point, while the push-pull controller acts when the reactor temperature reaches the switching points. Consequently the amplitude of the reactor temperature swings is smaller under PI control at the expense of more frequent valve actions.

Forced periodic control with multiple oscillating inputs

Experiments have been performed to study the effects of variations in oscillation frequency and in phase shift at various residence times. The oscillation amplitudes have been kept at the maximum values since earlier studies (Çinar et al., 1987a) confirmed that increasing the amplitude moves the upper branch of the average temperature curve away from the upper steady state loci of the system with fixed inputs, enabling stabilized operation in the unstable steady state region. Also, the nonsymmetric rectangular waveform has been used in the experimental studies since it is more effective than sinusoidal forcing functions (Çinar et al., 1987a) and much easier to implement.

Experimental results at various frequencies, phase shifts, and residence times, Figure 10, confirmed that stabilized reactor operation can be achieved with multiple oscillating inputs. The unforced reactor temperature is shown in Figure 10 at $t = 0$ s for each experiment. The amplitudes of the reactor temperature swings were much smaller than the amplitudes observed with oscillations in one input and often they were smaller than the amplitudes observed in feedback control experiments. Experiments at high frequency ($\omega = 8$) were conducted at two different phase shifts. At $\sigma = -0.15$, a reduction in residence time did not result in a large reduction in reactor temperature oscillations, Figure 10a, b, c. At $\sigma = -0.20$ the reduction in temperature swings was much more pronounced when the residence time was decreased from $\tau = 22$ s to $\tau = 20$s, Figure 10d, e, but at lower values ($\tau = 18$ s) the extinction of the reaction was observed and the system converged to the lower stable steady state, Figure 10f. As expected, at a lower frequency ($\omega = 5$), the reactor temperature had a larger amplitude of oscillation, Figures 10g, h, i. Again, the temperature oscillation amplitude was reduced with decreasing τ.

The average temperatures of the stabilized responses, Figure 11, agreed with the shape and location of the theoretical steady states, Figure 3c. Forced periodic operation indeed lowered the

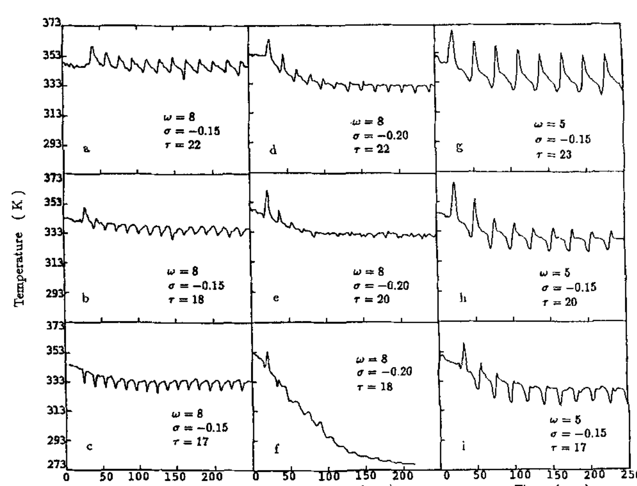

Figure 10. Forced periodic control of CSTR using input oscillations in flow rate and concentration.
$A_F = 1.66$; $A_C = 1.36$; $\alpha = 0.4$

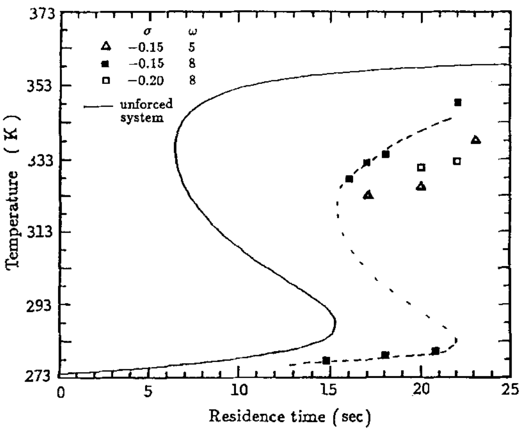

Figure 11. Average CSTR temperatures under forced periodic control with input flow rate and concentration oscillations.

$A_F = 1.66; A_C\ 1.36; \alpha = 0.4$

upper stable branch of the average temperature loci as shown in Figure 3 and permitted stabilized reactor operation in the unstable steady state region. For the operating conditions used, at a given temperature in the unstable steady state region, the average residence time under forced periodic control was greater than that of the system with fixed inputs. As discussed earlier, the closeness of the two residence times depends on the operating conditions, and the constraints of the experimental system did not permit experimental validation at the conditions where the two residence times coincide.

Disturbance rejection under forced periodic control has been assessed by instantaneous addition of 70 mL of water at 278 K to the reactor, Figure 12a, and by closure of the H_2O_2 valve for 6 s, Figure 12b. In both cases the system returned to the original stationary cycle.

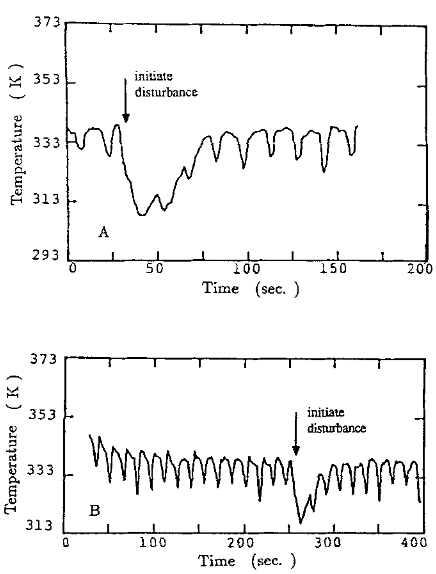

Figure 12. Effect of disturbances under forced periodic control with phase shift.

A. Addition of 70 mL water

B. Closure of H_2O_2 valve

$A_F = 1.66; A_C = 1.36; \alpha = 0.4$

$\tau = 18; \omega = 8; \sigma = -0.15$

Conclusions

Stabilized reactor operation in the unstable steady state region is achievd by all of the control techniques used in this study. PI feedback and nonlinear feedback control provide the security of a closed-loop feedback. Forced periodic control, on the other hand, is an open-loop control strategy and would be of value when measurements are costly and difficult or involve long time delays. For some of the control techniques, the manipulated variable used has a strong effect on the behavior of the reactor system. Three manipulated variables—feed flow rate, feed concentrations, and coolant flow rate—have been considered. While manipulations in feed flow rate or concentration do not cause additional costs, manipulation of coolant flow rate necessitates the existence of a cooling system, which increases capital and operating costs. Consequently, both process constraints and process economics will influence the selection of the control strategy and manipulated variable.

All control techniques and manipulated variables, except PI control with coolant flow rate manipulation, form an asymptotically stable limit cycle instead of the unstable steady state of the uncontrolled system. This results in sustained oscillations in reactor temperature. Experimental results indicate that the amplitude of reactor temperature swings can be smaller under forced periodic control with multiple oscillating inputs than under PI or push-pull control with feed flow rate manipulation. Phase shifts between oscillating inputs have a strong influence on reactor behavior and the range of phase shift which improves the response must be determined.

The theoretical contribution of this paper is based on an asymptotic method for the analysis of nonlinear systems with fast parametric oscillations. Using this method, techniques have been developed for assessing the effects of various parameters, such as forcing frequency and phase shift, on the behavior of a nonlinear system. The method and the techniques developed are general in nature. They can be used for a large class of chemical reactors modeled by ordinary differential equations, addressing not only the stabilization problem but also other relevant problems such as selectivity and yield improvement by forced periodic operation.

Acknowledgment

This work was supported by the U.S. Department of Energy under Grant No. DE-FG02-84ER13205. The authors are grateful to S. M. Meerkov for many stimulating discussions on vibrational control.

Notation

A_c, A_C, A_F, A_H = amplitude of oscillation of coolant flow, concentration, flow rate, heat transfer coefficient

B = dimensionless parameter group $\{-\Delta H\ c_{AF}\ \gamma\rho\ C_P\ T_F\ [1 + m_r C_r/(\rho\ C_P\ V)]\}$

b = ratio of stoichiometric coefficients $(Na_2S_2O_3/H_2O_2)$

c_A, c_B = hydrogen perioxide (A) sodium thiosulfate concentrations

C_P, C_r, C_{Pc} = heat capacity of reacting mixture, reactor material, coolant

ΔC = defined under Eq. 16

Da = Damkohler number, $c_{AF}\, k_0 \exp(-\gamma)\tau$

d_c = $\exp(\gamma)/(\rho C_P V c_{BF} k_0)$

E = activation energy

F = flow rate

H = effective heat transfer coefficient
ΔH = heat of reaction
K_c = feedback controller gain
k_0 = reaction rate constant
m_r = mass of solid material in contact with reacting material
p = ratio of feed concentrations, c_{AF}/c_{BF}
Q = energy removed by cooling coil
$Q_{i-1,2,3}(z_3)$ = defined under Eq. 13
$Q_0(x_3)$ = defined under Eq. 2
q_c = coolant flow rate
R = universal gas constant
S = defined under Eq. 13
T = period of oscillation
T_c = coolant temperature
T_r = reactor rise time
T' = reactor temperature
t', t = time, dimensionless time t'/τ
V = reactor volume
x_1 = dimensionless H_2O_2 concentration, $(c_{AF0} - c_A)/c_{AF0}$
x_2 = dimensionless $Na_2S_2O_3$ concentration, $(c_{BF0} - c_B)/c_{BF0}$
x_3 = dimensionless reactor temperature, $(T' - T_F)\gamma/T_F$
x_c = dimensionless coolant temperature, $(T_c - T_F)\gamma/T_F$
$X_1(\,), X_2(\,)$ = defined under Eq. 10
y_1, y_2, y_3 = dimensionless H_2O_2, $Na_2S_2O_3$ concentrations and temperature, respectively, in standard form
z_1, z_2, z_3 = average dimensionless H_2O_2, $Na_2S_2O_3$ concentrations and temperature, respectively, in oscillatory operation

Greek letters

α = duty fraction of nonsymmetric rectangular pulse
α_F = parameter ϵ/A_F
β'_k, β_k = defined under Eqs. 6, 13
γ = dimensionless activation energy, $E/(RT_F)$
$\gamma_\alpha, \gamma_\sigma$ = defined under Eq. 13
ϵ = parameter $1/T_r\omega$
θ = fast time t/ϵ
λ = dimensionless group $1/[1 + m_rC_r/(\rho C_P V)]$
μ_k = defined under Eq. 9
ν_k = defined under Eq. 9
ξ = defined under Eq. 14
ρ, ρ_c = density of reacting mixture, coolant
σ = phase shift
τ = residence time V/F
τ_I = feedback controller reset time
ω', ω = frequency, dimensionless frequency ($\omega = \omega'\tau$)

Subscripts

c = coolant property
F = feed state
m = minimum value
M = maximum value
o = average value
S = steady state
s = switching value

Literature Cited

Barshad, Y., and E. Gulari, "A Dynamic Study of CO Oxidation on Supported Platinum," *AIChE J.*, **31**(4), 649 (April 1985).

———, "Modification of Product Distribution through Periodic Operation: Fisher-Tropsch Synthesis over Ru/Al_2O_3," *Chem. Eng. Commun.*, **43**, 39 (1986).

Bellman, R., J. Bentsman, and S. M. Meerkov, "Nonlinear Systems with Fast Parametric Oscillations," *J. Math. Anal. Appl.*, **97**, 572 (1983).

———, "Vibrational Control of Nonlinear Systems: Vibrational Stabilizability," *IEEE Trans. Auto. Control,* **AC-31,** 710 (1986a).

———, "Vibrational Control of Nonlinear Systems: Vibrational Controllability and Transient Behavior," *IEEE Trans. Auto. Control,* **AC-31,** 717 (1986b).

Bentsman, J., and H. Hvostov, "Vibrational Control of a Laser-Illuminated Thermochemical System," *Proc. 1987 Am. Control Conf.*, **3,** 2072 (1987).

Bogoliubov, N. N., and Yu. A. Mitropolsky, *Asymptotic Methods in the Theory of Nonlinear Oscillations,* Gordon and Breach, New York (1961).

Bruns, D. D., and J. E. Bailey, "Process Operation Near an Unstable Steady State Using Nonlinear Feedback Control," *Chem. Eng. Sci.*, **30,** 755 (1975).

———, "Nonlinear Feedback Control for Operating a Nonisothermal CSTR Near an Unstable Steady State," *Chem. Eng. Sci.*, **32,** 257 (1977).

Chang, M., and R. A. Schmitz, "An Experimental Study of Oscillatory States in a Stirred Reactor," *Chem. Eng. Sci.*, **30,** 21 (1975a).

———, "Feedback Control of Unstable States in a Laboratory Reactor," *Chem. Eng. Sci.*, **30,** 837 (1975b).

Çinar, A., J. Deng, S. M. Meerkov, and X. Shu, "Vibrational Control of an Exothermic Reaction in a CSTR: Theory and Experiments," *AIChE J.*, **33,** (3), 353 (March 1987a).

Çinar, A., K. Rigopoulos, S. M. Meerkov, and X. Shu, "Vibrational Control of Chemical Reactors: Stabilization and Conversion Improvement in an Exothermic CSTR," *Chem. Eng. Commun.*, **59,** 299 (1987b).

Cutlip, M. B., "Concentration Forcing of Catalytic Surface Rate Processes," *AIChE J.*, **25** (5), 502 (May 1979).

Deng, J., "Experimental Application of Vibrational Control to an Exothermic Reaction in an Adiabatic CSTR," M.S. Thesis, Ill. Inst. Technol., Chicago (1985).

Jain, A. K., P. L. Silveston, and R. R. Hudgins, "Forced Composition Cycling Experiments in a Fixed-bed Ammonia Synthesis Reactor," *Am. Chem. Soc. Symp. Ser.*, **196,** 97 (1982).

Kevrekidis, I. G., L. D. Schmidt, and R. Aris, "Some Common Features of Periodically Forced Reacting Systems," *Chem. Eng. Sci.*, **41,** 1263 (1986).

Lyberatos, G., and S. A. Svoronos, "Optimal Periodic Square-Wave Forcing: A New Method," *Proc. 1987 Am. Control Conf.*, **1,** 257 (1987).

Meerkov, S. M., "Principle of Vibrational Control: Theory and Applications," *IEEE Trans. Auto. Control,* **AC-25,** 755 (1980).

———, "Conditions of Vibrational Stabilizability for a Class of Nonlinear Systems," *IEEE Trans. Auto. Control,* **AC-27,** 485 (1982).

Rigopoulos, K., "Vibrational Control Applications on a CSTR with an Exothermic Reaction," M.S. Thesis, Ill. Inst. Technol., Chicago (1986).

Silveston, P. L., R. R. Hudgins, A. A. Adesina, G. S. Ross, and J. L. Feimer, "Activity and Selectivity Control Through Periodic Composition Forcing over Fisher-Tropsch Catalysts," *Chem. Eng. Sci.*, **41,** 923 (1986).

Sincic, D., and J. Bailey, "Analytic Optimization and Sensitivity Analysis of Forced Periodic Chemical Processes," *Chem. Eng. Sci.*, **35,** 1153 (1980).

Watanabe, N., H. Kurimoto, M. Matsubara, and K. Onogi, "Periodic Control of Continuous Stirred Tank Reactors. II," *Chem. Eng. Sci.*, **37,** 745 (1982).

Wilson, H. D., and R. G. Rinker, "Concentration Forcing in Ammonia Synthesis—Controlled Cyclic Operation," *Chem. Eng. Sci.*, **37,** 343 (1982).

Manuscript received Oct. 30, 1987, and revision received July 15, 1988.